Current Topics

Action of Antimicrobial Peptides: Two-State Model[†]

Huey W. Huang*

Department of Physics, Rice University, Houston, Texas 77251

Received April 25, 2000; Revised Manuscript Received May 26, 2000

ABSTRACT: The argument and experimental evidence are presented for a two-state model that explains the action of both helical and β-sheet antimicrobial peptides after they bind to the plasma membranes of cells. Each peptide has two distinct physical states of binding to lipid bilayers. At low peptide-to-lipid ratios (P/L), the peptide tends to adsorb in the lipid headgroup region in a functionally inactive state. At a P/L above a threshold value P/L^*, the peptide forms a multiple-pore state that is lethal to a cell. The susceptibility of a cell to an antimicrobial peptide depends on the value of P/L^* that is determined by the lipid composition of the cell membrane. This model provides plausible explanations for the experimental findings that the susceptibility of different bacteria to a peptide is not directly correlated to its binding affinity, different peptides preferentially kill different pathogens, and peptides exhibit varying levels of lytic activity against different eukaryotic cells.

Gene-encoded peptide antibiotics are ubiquitous components of host defenses in mammals, birds, amphibia, insects, and plants (*1*). Because the activation and deployment of pathogen-specific immune responses occur slowly relative to the potential kinetics of microbial proliferation, epithelial surfaces and phagocytic cells are equipped with various broad spectrum antimicrobial substances that act rapidly to neutralize a broad range of potentially pathogenic microbes. Small endogenous antimicrobial peptides are stored in granules or vesicles which can be released or fused quickly into a phagosome, or they can be synthesized and excreted very rapidly after induction in certain types of cells, thus allowing them to play an important role in the initial phases of resistance to microbial invasion. For example, recent experiments suggest that a functional deficiency of endogenous antimicrobial peptides may contribute to the persistent airway infections seen in patients with cystic fibrosis (*1−3*).

Antimicrobial peptides are typically 20−40 amino acids in length, with a folded size approximating the membrane thickness. All evidence indicates that antimicrobial peptides act by permeabilizing the cell membranes of microorganisms (see reviews in ref *4*), although, in addition, receptor-mediated signaling activities of some peptides have been reported (*5*, *6*). The first indications that the peptides target the membranes were their wide spectrum of activity and their speed of action, often within minutes in vitro. Subsequently, all-D amino acid enantiomers of various peptides were synthesized and exhibited the same antimicrobial activities as their all-L native peptide counterparts (*7−10*). This implies that the action of antimicrobial peptides does not involve stereospecific protein receptors; rather, the action is the result of direct interaction with the lipid matrix of the membranes. However, such interactions are generally considered to be nonspecific. How do the defense mechanisms distinguish species self from infectious nonself? In this article, I will discuss the issue of specificity in peptide−lipid interactions that might be related to the target cell specificities exhibited by antimicrobial peptides.

* To whom correspondence should be addressed: Department of Physics, Rice University, Houston, TX 77251-1892. Telephone: (713) 348-4899. Fax: (713) 348-4150. E-mail: hwhuang@rice.edu.

Specificity or selective interaction of a protein is usually referred to the differential binding affinities of the protein to its targets. The function of the protein presumably follows the binding. Likewise, the first step of interaction between an antimicrobial peptide and a membrane is the physical binding of the peptide to the membrane surface. (Here we assume that the membrane is a cell's plasma membrane. How the peptides pass through the bacterial cell walls is another subject of research.) In this process, the electrostatic attraction apparently plays an important role (*11*, *12*). It is well-known that bacterial membranes contain negatively charged lipids on the outer leaflet, whereas the outer leaflets of eukaryotic cell membranes are predominantly neutral (*13*). And despite their diversity in structure, most antimicrobial peptides are positively charged. Thus, electrostatic interaction can be viewed as playing a regulatory role in target cell selectivity, i.e., differentiating microorganisms from eukaryotic cells. This has been a well-accepted concept since the antimicrobials were discovered (see reviews in ref *4*). However, we believe that there is at least one other regulatory step in the peptides' antimicrobial activity that occurs after binding to the membrane. One apparent reason to suspect that the charge on membrane is not the sole factor determining the peptides' efficacy is the fact that different peptides preferentially kill different pathogens (*6*, *14*). This cannot be the result of one cationic peptide being preferentially attracted to one group of pathogens while another cationic peptide is preferentially attracted to another group. For a similar reason, transmembrane electric potential is not likely a significant factor affecting the selectivity of peptides' action. Furthermore, the peptides exhibit varying levels of lytic activity against different eukaryotic cells. For example, the porcine peptide protegrin-1 is hemolytic for human erythrocytes but not for those of pigs or ruminants (private communications from R. I. Lehrer). Such differential susceptibilities of mammalian cells cannot be understood in terms of differences in the binding affinity to the peptide.

A general picture of how antimicrobial peptides behave after binding to a lipid bilayer was obtained from extensive experiments with magainin 2 (*15*−*19*), magainin analogue MSI-78 (*20*), protegin-1 (*21*, *22*), protegrin analogue IB367 (unpublished experiments), and two membrane active toxin/antimicrobials: alamethicin (*23*−*29*) and melittin (*30*). Their amino acid sequences are as follows: magainin 2, GIGKF[5]-LHSAK[10]KFGKA[15]FVGEI[20]MNS-CONH$_2$; MSI-78, GIGKF[5]-LKKAK[10]KFGKA[15]FVKIL[20]KK-CONH$_2$; protegrin-1 (PG-1), RGGRL[5]CYCRR[10]RFCVC[15]VGR-CONH$_2$; IB367, RGGLC[5]YCRGR[10]FCVCV[15]GR-CONH$_2$; alamethicin I, Ac-UPUAU[5]AQUVU[10]GLUPV[15]UUEQ-Phol; melittin, GIGAV[5]-LKVLT[10]TGLPA[15]LISWI[20]KRKR[25]QQ-CONH$_2$, where alamethicin is acetylated at the N-terminus (Ac) and its C-terminal residue is L-phenylalaninol (Phl), and Aib is α-aminoisobutyric acid. Alamethicin is the only peptide listed above that is not cationic. In fact, at physiological pH, alamethicin has a charge of −1. Four of these peptides, magainins 2, magainin analogue MSI-78, alamethicin, and melittin, fold into largely helical conformations upon binding to lipid bilayers. On the other hand, PG-1 folds into a β-hairpin stabilized by two disulfide bonds, according to solution NMR analyses (*31*, *32*). The conformation of IB367 is expected to be similar to PG-1,[1] on the basis of their analogy in amino acid sequence and the similarity between

their CD spectra (ref *21* and unpublished experiments). Despite their differences in the secondary structure, the overall shape of each peptide, with the side chains filling the space, is roughly cylindrical. The most important common characteristic of these peptides is that the folded cylindrical structures are hydrophobic on one side along the cylindrical axis and hydrophilic on the other. Thus, the minimum free energy configuration of a single peptide by itself is adsorbing on the bilayer's hydrophilic−hydrophobic interface with the cylindrical axis more or less parallel to the plane of the bilayer.

Two-State Model

Oriented circular dichroism (OCD) is a convenient method for detecting the configuration as well as the orientation of peptides bound to lipid bilayers (*23*). All the helical peptides we have investigated exhibit two distinct OCD spectra, depending on the peptide concentration [expressed as the molar peptide-to-lipid ratio (*P/L*)]. At low *P/L*'s, the OCD spectrum corresponds to a helical orientation parallel to the plane of the bilayers (*15*, *24*, *29*). However, above a threshold concentration *P/L**, whose value depends on the lipid composition of the bilayer, the OCD spectrum changes to one that corresponds to a helical orientation perpendicular to the plane of the bilayers. Concentration is not the only parameter that influences the peptide spectrum. For example, by varying the level of hydration of the peptide/lipid sample, one can change the OCD from one distinct spectrum to another through coexistence states, reversibly and continuously. Clearly helical peptides can exist in two distinct physical states in lipid bilayers; in one the helical orientation is parallel and in another perpendicular to the bilayer. Surprisingly, the β-sheet peptide protegrins also exhibit two distinct OCD spectra (*21*). However, unlike the case of helical peptides, there is no theoretical basis for interpreting the OCD of β-sheet peptides. Nevertheless, if we make a one-to-one correspondence between the two distinct OCD spectra of β-sheets and the two distinct OCD spectra of α-helices, the *P/L* versus the hydration phase diagram of PG-1 is exactly parallel to that of alamethicin (*21*). We called the state observed at low *P/L*'s the "S" state and the state observed at *P/L*'s above the threshold *P/L** the "I" state, for both α-helical and β-sheet peptides. We proposed that the action of antimicrobial peptides is effected by the transition from the S state to the I state. This two-state model has now accumulated a body of substantial evidence.

Multiple-Pore State

From the beginning, the pioneers of the field had conjectured that antimicrobial peptides kill microorganisms by making transmembrane pores (see reviews in ref *4*). Dissipation of the electric potential across energy-transducing membranes (*33*) and ion conductance across lipid bilayers caused by the peptides (*34*−*36*) were explained by formation of ion channels or pores. The passage of ions would lower the proton gradient and destroy the membrane potential, stopping ATP production and all cellular metabolism, and the cell would die. Peptide-induced leakage from vesicles (*14*, *37*, *38*) reinforced the image of pore formation.

---

[1] Abbreviations: *P/L*, molar ratio of bound peptide to lipid; PG-1, protegrin-1; OCD, oriented circular dichroism; PC, phosphatidylcholine; PE, phosphatidylethanolamine.
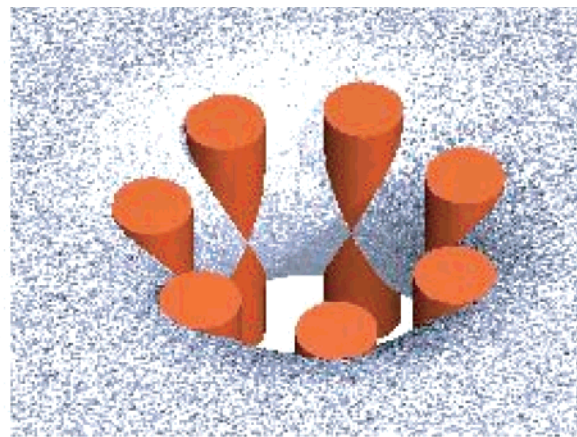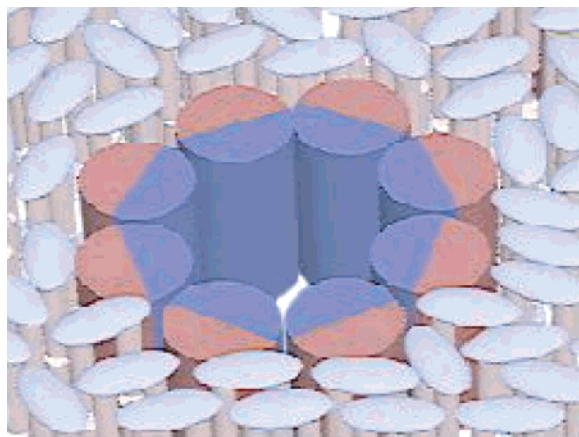
FIGURE 1: Barrel-stave model for alamethicin and toroidal model for magainin pores (*17*, *27*). (Left) Alamethicin monomers are represented by cylinders that are ~11 Å in diameter; blue and red represent hydrophilic and hydrophobic sides of the amphiphilic peptide, respectively. The diameter of the water pathway (pore) is ~18 Å. The lipid molecule is represented by an oval headgroup with two legs. (Right) Magainin monomers are represented by orange cylinders embedded in the lipid headgroup region. The gray surface represents the surface of the lipid headgroups. The surface bends continuously from the top leaflet to the bottom leaflet like the inside of a torus. The bending expands the headgroup region relative to the chains. The expanded space is filled by magainin monomers (see details in ref *17*). The diameter of the pore is ~30 Å.

However, a direct detection of the pores in membranes with structural information has been difficult. Without labeling, a peptide pore in a lipid bilayer does not provide sufficient contrast in either electron density or neutron scattering-length density to be detectable by X-ray, electron, or neutron diffraction. We solved this contrast problem by replacing water with D_2O. If there are water-filled pores in the membrane, the replacement of water with D_2O within the pores will provide a strong contrast in neutron scattering-length density against the lipid bilayer so they can easily be detected by neutron diffraction (*26*). Perhaps the most apparent evidence for pore formation is the experiment showing that alamethicin and magainin each produced a neutron diffraction pattern similar to the one produced by the well-established transmembrane gramicidin channel (*19*). It is important to note that neutron samples can be directly inspected by OCD, because both experiments utilize samples deposited on a quartz substrate and quartz is permeable to neutrons as well as to ultraviolet. The pore-like diffraction patterns were detected only when the peptides were in the I state, not when they were in the S state (*17*, *27*). Also, pore-like diffraction patterns by PG-1 and IB367 have been detected recently (unpublished experiments). Thus, we identified the I state as the multiple-pore state. The pores formed by various peptides vary in size and structure (*17*, *18*, *27*), but all are ≥20 Å in diameter, sufficient for passage of small ions and molecules. The peptide concentrations at which the pores were observed by neutron diffraction are about $^1/_2$ of those required for 50% killing in bacterial killing assays, where radioactivity binding experiments showed that the amount of bound peptide was roughly equivalent to the amount needed for forming a monolayer around that bacterium (assuming 350 Å^2 per peptide) (*14*, *39*). Under such conditions, the pore concentrations are high (the water holes occupy about 10% of the membrane area in the neutron samples) and the multiple-pore states are stable, at least statistically, as evidenced by the neutron diffraction patterns. Whether individual pores have a finite lifetime (*11*) is irrelevant to the action exerted by a high peptide concentration.

The pores described above were observed in the fluid state of lipid bilayers (*17*, *18*, *27*), presumably similar to the physiological condition of cell membranes (*13*). The diffraction data from the fluid state gave a reliable measurement for the pore size (ca. ±1 Å). But the signals were limited to a low range of *q* (the momentum transfer of scattering), so they would not allow detailed structural analyses of the pores. In the case of alamethicin, the pore size and the peptide/lipid ratio were consistent with the barrel-stave model (see Figure 1) that was proposed earlier on the basis of single-channel conduction analyses (*40*, *41*). The proposed toroidal model for the magainin pores (see Figure 1) (*17*) was constructed on the basis of indirect evidence, including the pore size, the pore density, the peptide-to-lipid ratio, the orientation of the peptide, and an important constraint that magainin is always associated with the lipid headgroups rather than with the chains. This constraint was given by a wide range of experiments, including Raman (*42*), fluorescence (*43*), differential scanning calorimetry (*38*), and NMR (*44*). The toroidal model in which the lipid headgroups and magainins together line the inside of the pore is consistent with all available data reported so far. An equivalent model was independently proposed by Matsuzaki et al. (*45*) on the basis of the observation that the flip-flop rate of lipid between leaflets of the membrane increased during the leakage experiment from vesicles. However, this argument for the toroidal model may not be compelling, because a similar increase in the flip-flop rate was observed during the alamethicin conductance (*46*).

Recently, we have successfully crystallized the multiple-pore states of magainin and protegrin in membranes (unpublished experiments). We are hopeful that crystallographic diffraction of these crystalline phases will reveal structural information about the pores. Interestingly, the same crystallization procedure failed to crystallize the multiple-pore state of alamethicin. Perhaps this is another indication that there is a fundamental difference between the alamethicin pore and the pores made by self-defense antimicrobial peptides.

Surface Adsorption State

The absence of pores indicates that the S state is a functionally inactive or nonproductive binding state (*14*). Peptides in this state have been investigated extensively. Solid-state NMR (*44*, *47*), Raman (*42*), fluorescence (*43*), and DSC (*38*) measurements all indicated that magainin is associated with the headgroups of the lipid bilayer, and the helical axis is oriented parallel to the interface. We have found by X-ray diffraction that peptides in this state cause membrane thinning; moreover, the amount of thinning is directly proportional to the peptide concentration P/L (*16*, *22*, *25*). This result is consistent with the peptides being embedded in the lipid headgroup region. The embedding stretches the area of the membrane. Since the volume of the hydrocarbon region is constant, the hydrocarbon thickness decreases in proportion to the areal increase, and, in turn, proportional to the peptide concentration P/L. Indeed, in all the cases, we have investigated, including alamethicin (*25*), magainin (*16*), and protegrin (*22*), we could deduce the area increment caused by each peptide and found it to be in agreement with the molecular size of the peptide.

Investigators have looked for peptide aggregation on the membrane surface as a precursory condition for pore formation. As far as we know, no aggregations have been detected (*44*, *48−50*). In a careful fluorescence energy transfer experiment, Schümann et al. (*50*) have shown that the magainin distribution on the membrane surface is not entirely random. Rather, they are randomly distributed with the provision that the distance of closest approach between two magainin molecules is ≥20 Å. This finding is in good agreement with a prediction based on the elasticity theory of lipid bilayers (*51*). As described above, peptide adsorption thins the bilayer locally. Such membrane distortion costs energy. Thus, the free energy of adsorption is the sum of two terms: a negative binding energy and a positive energy cost of bilayer deformation. This deformation energy is proportional to the square of the amplitude of the thinning, according to the elasticity theory. As a result of this square rule, the energy cost of bilayer deformation *increases* if two initially far-separated surface-adsorbed peptides aggregate (*51*). [This is opposite from the case of two inserted peptides, where the energy cost of bilayer deformation will *decrease* by aggregation, as demonstrated experimentally and theoretically with gramicidin in thick bilayers (see refs *52* and *53*).] The repulsive force between two surface-adsorbed peptides extends over a separation distance of about 25 Å (*51*). Beyond this range of repulsion, the peptide distribution should be random. We note that even in the pores, magainins are separated by lipid headgroups as predicted by the toroidal pore model (see Figure 1; *17*, *45*). Thus, the absence of close association between peptide monomers (*44*, *48−50*) is totally consistent with the two-state model.

Mechanism of Transition

The presence of a transmembrane electric potential can lower the free energy of the insertion state relative to the surface adsorption state for peptides possessing a dipole moment, such as the case of helical peptides. However, transmembrane potential cannot explain the transition from the S state to the I state as a function of peptide concentration. Furthermore, some peptides such as PG-1 appear to have

no dipole moment (*54*), so the transmembrane potential cannot be a key factor for the action of protegrin-like peptides. One possible explanation for the concentration-dependent transition is found in the energy cost of bilayer thinning caused by the peptide adsorption in the S state. Since the thinning is proportional to P/L, the energy cost is proportional to $(P/L)^2$. Thus, although the energy of surface adsorption starts with a negative binding energy, it increases with a positive term proportional to $(P/L)^2$. While at low peptide concentrations the energy level of the surface adsorption state is lower than that of the pore state, at sufficiently high peptide concentrations, the former eventually exceeds the latter and, hence, the transition from the S state to the I state at a high P/L.

Such a transition need not involve an intermediate state. In the case of alamethicin, an analysis of single-channel conductances and state-transition kinetics by Mak and Webb (*41*) concluded that the peptide monomerically inserts transmembrane and then aggregates to form pores. However, a similar scenario for magainin is unlikely, because, as mentioned above, magainin has been found to be strongly associated with the lipid headgroups. One reason is that magainin has four positive charges on its hydrophilic side, so the free energy for monomeric transmembrane insertion must be high. (By contrast, alamethicin is essentially neutral.) Thus magainin appears to make direct transitions between the S state and the I state without an identifiable intermediate.

We note that if the toroidal model as depicted in Figure 1 were correct, the magainin channel could not exist outside of a lipid bilayer, because lipid headgroups are part of the channel. The barrel-stave model for alamethicin is also likely to be unstable without the support of the lipid bilayer, for example, if the lipid is replaced with detergent. Thus, the pores of antimicrobial peptides are fundamentally different from the pores formed by proteins 1 order of magnitude larger, such as *Staphylococcus aureus* α-hemolysin (*55*). α-Hemolysin is secreted as a 33.2 kDa water-soluble monomer. Membrane-bound monomers assemble via a heptameric prepore intermediate to form a transmembrane pore. The crystalline structure of the detergent-solubilized pore shows that the heptameric structure is stabilized by extensive intermonomer interactions (*53*) that could not occur between parallel helices in a barrel-stave model.

According to our theory of transition, the threshold value P/L^* is the peptide concentration when the energy levels of the S state and the I state are equal. Therefore, P/L^* is a function of the adsorption binding energy, the elastic constants of the bilayer, and the energy level of the pore state, which all vary with the lipid composition of the bilayer. Other factors that may vary P/L^* include transmembrane electric potential and perhaps the pH level which influences the charge state of peptides. Thus, P/L^* will vary greatly with the lipid composition and the physicochemical condition of the membrane, as shown by experiments (*15*, *21*, *24*, *29*). Matsuzaki et al. (*56*) pointed out that the peptide embedded in the headgroup region imposes positive curvature strain that apparently facilitates the formation of toroidal pores; therefore, the presence of negative curvature-inducing lipids would inhibit pore formation. While this idea is qualitatively correct, it is difficult to put it in a quantitative form.

A simple example of lipid dependence can be understood in terms of the membrane thinning effect described above.

When the size of the lipid headgroup is reduced while the chains remain the same, e.g., replacing PC with PE lipids, the strain to the bilayer, i.e., the thinning, caused by peptide adsorption is lessened, and thus, the threshold P/L^* increases according to the simple geometric relation $(P/L^*)_\theta = (P/L^*)_{\theta=0} + \theta(\Sigma_{PC} - \Sigma_{PE})/\Gamma$ (29), where θ is the fraction of PE in the PC/PE mixture, Σ_{PC} and Σ_{PE} are the cross-sectional areas of PC and PE headgroups, respectively, and Γ is the cross-sectional area of the peptide along its cylindrical axis. This prediction was confirmed by experiment (29). Thus, it provides a possible explanation for why protegrins are toxic to human erythrocytes (which are rich in PC lipids; 57) but nontoxic to those of pigs (which are rich in PE lipids; 58). Given the same peptide concentration P/L, cells with low P/L^*'s will be lysed while the cells with high P/L^*'s may survive. Following this logic, it is not surprising that all-D amino acid enantiomers have the same antimicrobial spectra as their all-L native peptide counterparts (7−10). Even an unnatural β-amino acid oligomer has been synthesized to mimic the antimicrobial activity of a magainin (59).

We conclude that the charge on the membrane is the first regulatory factor in target cell specificity, but the variation of P/L^* by lipid composition is an equally important second regulatory factor that determines the susceptibility of a cell to an antimicrobial peptide. This second regulatory mechanism provides a possible explanation for the experimental findings that the susceptibility of different bacteria to a peptide is not directly correlated to its binding affinity (14), different peptides preferentially kill different pathogens (6, 14), and peptides exhibit varying levels of lytic activity against different eukaryotic cells. What remain to be shown are the quantitative correlations between the killing assays and the lipid dependence of P/L^*. The problem can also be complicated by the effects of cell walls which are yet to be systematically investigated.

ACKNOWLEDGMENT

REFERENCES

1. Martin, E., Ganz, T., and Lehrer, R. I. (1995) *J. Leukocyte Biol. 58*, 128−136.
2. Smith, J. J., Travis, S. M., Greenberg, E. P., and Welsh, M. J. (1996) *Cell 85*, 229−236.
3. Goldman, M., Anderson, G., Stolzenberg, E. D., Kari, U. P., Zasloff, M., and Wilson, J. M. (1997) *Cell 88*, 553−560.
4. Boman, H. G., Marsh, J., and Goode, J. A., Eds. (1994) *Antimicrobial Peptides*, Ciba Foundation Symposium 186, pp 1−272, John Wiley & Sons, Chichester, U.K.
5. Yang, D., Chertov, O., Bykovskaia, S. N., Chen, Q., Buffo, M. J., Shogan, J., Anderson, M., Schroder, J. M., Wang, J. M., Howard, O. M. Z., and Oppenheim, J. J. (1999) *Science 286*, 525−528.
6. Hoffmann, J. A., Kafatos, F. C., Janeway, C. A., and Ezekowitz, R. A. B. (1999) *Science 248*, 1313−1318.
7. Wade, D., Boman, A. Wåhlin, B., Drain, C. M., Andreu, D., Boman, H. G., and Merrifield, R. B. (1990) *Proc. Natl. Acad. Sci. U.S.A. 87*, 4761−4765.
8. Bessalle, R., Kapitkovsky, A., Gorea, A., Shalit, I., and Fridkin, M. (1990) *FEBS Lett. 274*, 151−155.
9. Yasin, B., Lehrer, R. I., Harwig, S. S. L., and Wagar, E. A. (1996) *Infect. Immun. 64*, 4863−4866.
10. Cho, Y., Turner, J. S., Dinh, N., and Lehrer, R. I. (1998) *Candida albicans. Infect. Immun. 66*, 2486−2493.
11. Matzuzaki, K., Sugishita, K., Harada, M., Fujii, N., and Miyajima, K. (1997) *Biochim. Biophys. Acta 1327*, 119−130.
12. Lohner, K., Latal, A., Lehrer, R. I., and Ganz, T. (1997) *Biochemistry 36*, 1525−1531.
13. Gennis, R. B. (1989) *Biomembranes*, pp 151−158, Springer-Verlag, New York.
14. Steiner, H., Andreu, D., and Merrifield, R. B. (1988) *Biochim. Biophys. Acta 939*, 260−266.
15. Ludtke, S. J., He, K., Wu, Y., and Huang, H. W. (1994) *Biochim. Biophys. Acta 1190*, 181−184.
16. Ludtke, S. J., He, K., and Huang, H. W. (1995) *Biochemistry 34*, 16764−16769.
17. Ludtke, S. J., He, K., Heller, W. T., Harroun, T. A., Yang, L., and Huang, H. W. (1996) *Biochemistry 35*, 13723−13728.
18. Yang, L., Harroun, T. A., Heller, W. T., Weiss, T. M., and Huang, H. W. (1998) *Biophys. J. 75*, 641−645.
19. Yang, L., Weiss, T. M., Harroun, T. A., Heller, W. T., and Huang, H. W. (1999) *Biophys. J. 77*, 2648−2656.
20. Maloy, W. L., and Kari, U. P. (1995) *Biopolymers 37*, 105−122.
21. Heller, W. T., Waring, A. J., Lehrer, R. I., and Huang, H. W. (1998) *Biochemistry 37*, 17331−17338.
22. Heller, W. T., Waring, A. J., Lehrer, R. I., Harroun, T. A., Weiss, T. M., Yang, L., and Huang, H. W. (2000) *Biochemistry 39*, 139−145.
23. Wu, Y., Huang, H. W., and Olah, G. A. (1990) *Biophys. J. 57*, 797−806.
24. Huang, H. W., and Wu, Y. (1991) *Biophys. J. 60*, 1079−1087.
25. Wu, Y., He, K., Ludtke, S. J., and Huang, H. W. (1995) *Biophys. J. 68*, 2361−2369.
26. He, K., Ludtke, S. J., Worcester, D. L., and Huang, H. W. (1995) *Biochemistry 34*, 15614−15618.
27. He, K., Ludtke, S. J., Worcester, D. L., and Huang, H. W. (1996) *Biophys. J. 70*, 2659−2666.
28. He, K., Ludtke, S. J., Heller, W. T., and Huang, H. W. (1996) *Biophys. J. 71*, 2669−2679.
29. Heller, W. T., He, K., Ludtke, S. J., Harroun, T. A., and Huang, H. W. (1997) *Biophys. J. 73*, 239−244.
30. Harroun, T. A. (1999) Ph.D. Thesis, Rice University, Houston, TX.
31. Aumelas, A., Mangoni, M., Roumestand, C., Chiche, L., Despaux, E., Grassy, G., Calas, B., and Chavanieu, A. (1996) *Eur. J. Biochem. 237*, 575−583.
32. Fahrner, R. L., Dieckmann, T., Harwig, S. S. L., Lehrer, R. I., Eisenberg, D., and Feigon, J. (1996) *Chem. Biol. 3*, 543−550.
33. Westerhoff, H. V., Juretic, D., Hendler, R. W., and Zasloff, M. (1989) *Proc. Natl. Acad. Sci. U.S.A. 86*, 6597−6601.
34. Christensen, B., Fink, J., Merrifield, R. B., and Mauzerall, D. (1988) *Proc. Natl. Acad. Sci. U.S.A. 85*, 5072−5076.
35. Duchohier, H., Molle, G., and Spach, G. (1989) *Biophys. J. 56*, 1017−1021.
36. Sokolov, Y., Mirzabekov, T., Martin, D. W., Lehrer, R. I., and Kagan, B. L. (1999) *Biochim. Biophys. Acta 1420*, 23−29.
37. Matzuzaki, K., Harada, M., Handa, T., Fumakoshi, S., Fujii, N., Yajima, H., and Miyajima, K. (1989) *Biochim. Biophys. Acta 981*, 130−134.
38. Matzuzaki, K., Harada, M., Fumakoshi, S., Fujii, N., and Miyajima, K. (1991) *Biochim. Biophys. Acta 1063*, 162−170.
39. Merrifield, R. B., Merrifield, E. L., Juvvadi, P., Andreu, D., and Boman, H. G. (1994) in *Antimicrobial Peptides* (Boman, H. G., Marsh, J., and Goode, J. A., Eds.) Ciba Foundation Symposium 186, pp 5−26, John Wiley & Sons, Chichester, U.K.
40. Baumann, G., and Mueller, P. (1974) *J. Supramol. Struct. 2*, 538−557.
41. Mak, D. D., and Webb, W. W. (1995) *Biophys. J. 69*, 2323−2336.
42. Williams, R. W., Starman, R., Taylor, K. M. P., Cable, K., Beeler, T., Zasloff, M., and Covell, D. (1990) *Biochemistry 29*, 4490−4496.

43. Matsuzaki, K., Murase, O., Tokuda, H., Fumakoshi, S., Fujii, N., and Miyajima, K. (1994) *Biochemistry 33*, 3342−3349.

44. Hirsh, D. J., Hammer, J., Maloy, W. L., Blazyk, J., and Schaefer, J. (1996) *Biochemistry 35*, 12733−12741.

45. Matsuzaki, K., Murase, O., Tokuda, H., Fujii, N., and Miyajima, K. (1996) *Biochemistry 35*, 11361−11368.

46. Hall, J. E. (1981) *Biophys. J. 33*, 373−381.

47. Bechinger, B., Kim, Y., Chirlian, L. E., Gesell, J., Neumann, J.-M., Motal, M., Tomich, J., Zasloff, M., and Opella, S. J. (1991) *J. Biol. NMR 1*, 167−173.

48. Gazit, E., Lee, W. J., Brey, P. T., and Shai, Y. (1994) *Biochemistry 33*, 10681−10692.

49. Gazit, E., Boman, A., Boman, H., and Shai, Y. (1995) *Biochemistry 34*, 11479−11488.

50. Schümann, M., Dathe, M., Wieprecht, T., Beyermann, M., and Bienert, M. (1996) *Biochemistry 36*, 4345−4351.

51. Huang, H. W. (1995) *J. Phys. II 5*, 1427−1431.

52. Harroun, T. A., Heller, W. T., Weiss, T. M., Yang, L., and Huang, H. W. (1999) *Biophys. J. 76*, 937−945.

53. Harroun, T. A., Heller, W. T., Weiss, T. M., Yang, L., and Huang, H. W. (1999) *Biophys. J. 76*, 3176−3185.

54. Hol, W. G. J., Halie, L. M., and Sander, C. (1981) *Nature 294*, 532−536.

55. Song, L., Hobaugh, M. R., Shustak, C., Cheley, S. Bayley, H., and Gouaux, J. E. (1996) *Science 274*, 1859−1865.

56. Matsuzaki, K., Sugishita, K., Ishibe, N., Ueha, M., Nakata, S., Miyajima, K., and Epand, R. M. (1998) *Biochemistry 37*, 11856−11863.

57. Nouri-Sorkhabi, M. H., Wright, L. C., Sullivan, D. R., and Kuchel, P. W. (1996) *Lipids 31*, 765−770.

58. Nouri-Sorkhabi, M. H., Agar, N. S., Sullivan, D. R., Gallagher, C., and Kuchel, P. W. (1996) *Comp. Biochem. Physiol. 113B*, 221−227.

59. Porter, E. A., Wang, X., Lee, H.-S., Weisblum, B., and Gellman, S. H. (2000) *Nature 404*, 565.